2009 IEEE International Conference on Robotics and Automation
Kobe International Conference Center
Kobe, Japan, May 12-17, 2009

Bouncing an Unconstrained Ball in Three Dimensions with a Blind Juggling Robot

Philipp Reist and Raffaello D'Andrea

***Abstract*— We describe the design of a juggling robot that is able to vertically bounce a completely unconstrained ball without any sensing. The robot consists of a linear motor actuating a machined aluminum paddle. The curvature of this paddle keeps the ball from falling off while the apex height of the ball is stabilized by decelerating the paddle at impact. We analyze the mapping of perturbations of the nominal trajectory over a single bounce to determine the design parameters that stabilize the system. The first robot prototype confirms the results from the stability analysis and exhibits substantial robustness to perturbations in the horizontal degree of freedoms. We then measure the performance of the robot and characterize the noise introduced into the system as white noise. This allows us to refine the design parameters by minimizing the H_2 norm of an input-output representation of the system. Finally, we design an H_2 optimal controller for the apex height using impact time measurements as feedback and show that the closed-loop performance is only marginally better than what is achieved with open-loop control.**

I. INTRODUCTION

We present a robot that can vertically juggle a single, completely unconstrained ball without any sensing and explain the process and analysis that led us to the design of the robot. The robot consists of a linear motor that actuates a machined aluminum paddle. Therefore, the robot stabilizes a ball in three dimensions with only one degree of freedom.

The paddle has a slightly concave parabolic shape which keeps the ball from falling off the robot. In addition, a decelerating paddle motion at impact stabilizes the apex height of the ball. We find suitable values for these two design parameters by analyzing the stability of the system for a range of apex heights and ball properties.

In order to analyze stability, we perform a perturbation analysis on the nominal trajectory of the ball over a single bounce from apex to apex. This analysis produces a linear mapping of the perturbations over a bounce. By studying the stability regions of this mapping over a range of apex heights and ball properties, we find suitable design parameter values for the first robot prototype. Using these values, the robot is able to continuously juggle a variety of balls at different heights. The robot also exhibits substantial robustness to perturbations in the horizontal degree of freedoms.

We evaluate the performance of the robot prototype using a video camera and an impact detector. We measure the impact times and impact locations during extended runs. Using the measurement results, we can estimate the deviations of the ball's post-impact velocities from the values predicted by the impact models. We characterize these deviations as a white noise input into the system. This allows us to refine the design parameters using the H_2 system norm. Roughly speaking, an interpretation of the H_2 norm is the gain of a system when the input is white noise [1]. After setting up an input-output model of the system, we are then able to find the optimal design parameters by minimizing the H_2 norm.

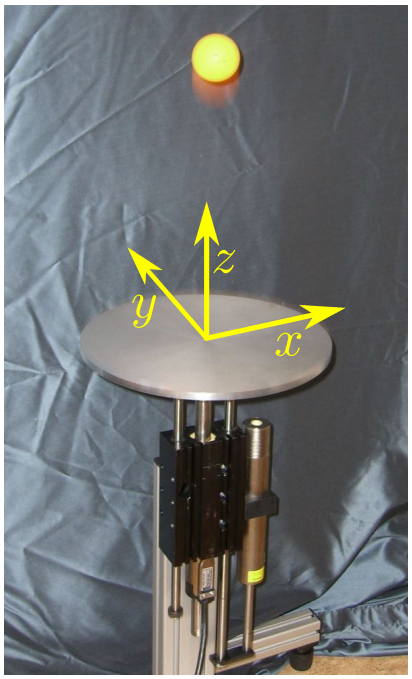

Fig. 1. The Blind Juggler. The origin of the coordinate system lies at nominal impact height and in the center of the paddle. The rotational degrees of freedom ω_x, ω_y are defined by the right-hand rule.

Finally, we design an H_2 optimal controller for the apex height using the measured impact time as feedback signal. The control input to the system is the deviation from the nominal impact state of the paddle. We compare the closed-loop to the open-loop H_2 norm and find that it only marginally improves. Therefore, actively controlling the apex height is not necessary.

The main contributions of this paper are extending the stability analysis of an underactuated, open-loop bouncing ball system to three dimensions including spin and confirming the results using a robot prototype. In order to achieve this, we present the novel strategy of stabilizing the ball by an appropriate paddle curvature.

The paper is structured as follows: First, we give an overview of related work. We then show the derivation of

P. Reist and R. D'Andrea are with the IMRT at ETH Zurich, Switzerland. Supporting material, including videos, may be found at `www.blindjuggler.org`.

the nominal trajectory of the ball in Section II. We perform the perturbation analysis yielding the linear mapping in Section III. Next, we choose the stabilizing design parameters in Section IV. In Section V, we discuss the experimental results obtained with the robot prototype and identify the noise parameters. We refine the design parameters by optimizing the H_2 norm of the system in Section VI, where we also present a performance comparison of the initial to the refined design. In Section VII, we derive the H_2 optimal controller for the apex height and compare the closed-loop and open-loop H_2 system norms.

A. Related Work

The bouncing ball system has received attention in dynamics, as it is a simple system that exhibits complex dynamical behaviors [2], [3]. In robotics, juggling has been studied as a challenging dexterous task. Bühler, Koditschek and Kindlmann were amongst the first to study robotic juggling and introduced a feedback law called the mirror algorithm [4]–[7]. The algorithm defines the trajectory of the paddle as a mirrored (about the desired impact height) and scaled version of the ball's trajectory. Consequently, this requires constant tracking of the ball's position. The authors showed that the apex height of the ball is stabilized. Interestingly, the resulting paddle trajectory is accelerating at impact, which contrasts the result of Schaal and Atkeson who analyzed the stabilizing property of a decelerating paddle for an open-loop bouncing ball system [8].

Recently, Ronsse et al. have been studying different juggling systems; in particular a ball-in-wedge system [9]–[12]. The authors introduced the term "blind" juggling robot in [12], where they present a planar ball-in-wedge juggling robot that is able to juggle purely feed-forward or with feedback using measured impact times. It is even able to generate a juggling pattern similar to the popular shower pattern (you may watch a video they refer to in [12] or on the first author's homepage).

In [11], [12], Ronsse also addressed robustness of the bouncing ball system to static and dynamic errors in the ball's coefficient of restitution (*CR*). The authors first derived the transfer function of the errors in the *CR* to the post-impact velocity perturbations. Then, they placed the zero of the transfer function by adjusting the paddle acceleration to either compensate for static or dynamic errors. This is a similar strategy to the H_2 noise-to-output minimization we use to find optimal design parameters.

In the literature, juggling robots mostly juggle constrained balls that have only one [13]–[15] or two [4]–[7], [9]–[12] translational degrees of freedom. Robots juggling unconstrained balls in three dimensions also have been implemented. They all feature a robotic arm [16]–[19] that actively controls all the ball's degrees of freedom. These more complex robots rely on continuous tracking of the ball's position using cameras. Schaal and Atkeson present in [8] an open-loop juggling robot that features a paddle which passively keeps the ball in its center: they used a trampoline-like racket to stabilize the horizontal degrees of freedom of the ball. However, their focus lies on the analysis of the vertical stability of the ball.

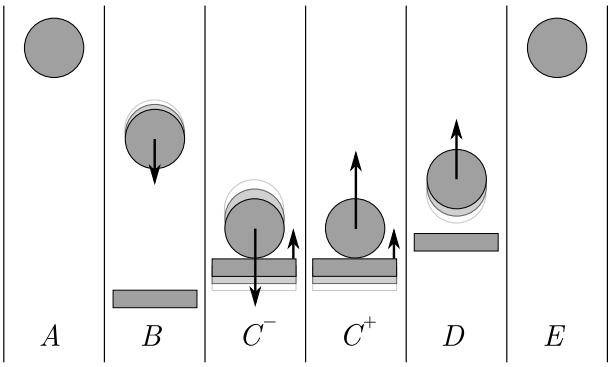

Fig. 2. Nominal Trajectory

In legged robotics, the equivalent of a bouncing ball system is a hopping robot. Ringrose presents in [20] the design of a self stabilizing monopod featuring a curved foot. After proving that the hopping height is open-loop stable, the author determines the foot radius based on a stability analysis of the robot's pitch. This passive stabilization of the hopper's height and pitch is similar to bouncing a ball on a parabolic plate without any sensing.

II. NOMINAL TRAJECTORY

Before we can perform a perturbation analysis on the system, we first have to establish the nominal trajectory, sketched in Fig. 2. Given some parameters, e.g. the *CR* of the ball and the nominal apex height, we want to find unknown parameters such as the nominal paddle speed at impact.

The ball starts at rest at the nominal apex height (*A*). It is then subject to free fall (*B*) before the impact with the paddle (*C*). Finally, the ball is subject to free fall (*D*) until it reaches the nominal apex height again (*E*). We develop the nominal trajectory in a general way and introduce general functions F, Δ and Γ that describe the ball dynamics during free fall, the impact condition and the state changes over impact, respectively. In Section III, we define the functions F, Δ and Γ and states for the Ball S and paddle P specific to the Blind Juggler.

A. Initial Ball State at Apex

$$\bar{S}\big(t = \bar{T}_0\big) = \bar{S}_0 \tag{1}$$

B. Free Fall until Impact

The ball falls freely for $\bar{T}_0 \leq t \leq \bar{T}_1$, where $\bar{T}_1$ is the nominal impact time. The fall is governed by

$$\dot{\bar{S}}(t) = F\left(\bar{S}(t)\right). \tag{2}$$

F captures the dynamics of the ball subject to free fall. The impact occurs if the impact condition described by Δ is satisfied:

$$\Delta\big(\bar{S}_1, \bar{P}_1\big) = 0, \tag{3}$$

where $\bar{S}_1$ and $\bar{P}_1$ are the nominal impact state of the ball and paddle, respectively.

C. Impact

The impact function Γ maps the pre-impact $(-)$ to the post-impact $(+)$ ball state, given the paddle state. It contains the impact parameters such as *CR* and geometrical parameters. We assume the impact to be instantaneous, i.e. $\bar{T}_1 = \bar{T}_2^- = \bar{T}_2^+$.

$$\begin{aligned} \bar{S}_2^- &= \bar{S}_1 \\ \bar{P}_2^- &= \bar{P}_1 \\ \bar{S}_2^+ &= \Gamma\big(\bar{S}_2^-, \bar{P}_2^-\big) \end{aligned} \tag{4}$$

D. Free Fall until Apex

After the impact, the ball is subject to free fall for $\bar{T}_2 \leq t \leq \bar{T}_3$. We can reuse (2) with different initial conditions

$$\bar{S}\big(\bar{T}_2\big) = \bar{S}_2^+ \tag{5}$$

$$\bar{S}_3 = \bar{S}\big(\bar{T}_3\big). \tag{6}$$

E. Boundary Condition and Solution

We require the boundary condition

$$\bar{S}_3 = \bar{S}_0. \tag{7}$$

With the above equations, we established a system of equations which we can solve for the nominal ball trajectory and the unknown parameters. For the Blind Juggler, we find

$$\bar{T}_1 = \sqrt{\frac{2H}{\gamma}} \qquad \bar{T}_3 = 2\bar{T}_1 \qquad \bar{v}_P = -\bar{v}_S \frac{1-e_z}{1+e_z}, \tag{8}$$

where H is the nominal apex height, γ is the gravitational acceleration and e_z is the vertical *CR*. $\bar{v}_P$, $\bar{v}_S$ are the paddle's and ball's nominal impact velocities, respectively. These results are straightforward. However, they are an important prerequisite for the following perturbation analysis. The general derivation further allows introducing more complex models for the impact, problem geometry, or free fall (for example, aerodynamic drag).

III. PERTURBATION ANALYSIS

In order to analyze the stability of the system, we derive a linear mapping which describes how perturbations added to the initial conditions of the nominal trajectory map over a single bounce. Since the perturbations are small, we can propagate them over the bounce using first order approximations to the system equations. The derived mapping allows us to find the stabilizing design parameters a_P, the paddle's acceleration at impact, and c, the curvature of the paddle.

We perform the analysis in the coordinate system shown in Fig. 1. The mapping is derived in two dimensions including spin. However, we show that the analysis generalizes to three dimensions. We can omit the y and ω_x degrees of freedom of the ball as we assume x, ω_y and y, ω_x to be uncorrelated. We present experimental results in Section V that confirm this assumption. Therefore, the ball state for the analysis is $S = (x, \dot{x}, \omega_y, z, \dot{z})$.

A. Introduce Perturbations

The perturbations s_0 are added to the nominal initial conditions of the ball.

$$S_0 = \bar{S}_0 + s_0 \qquad \|s_0\| \ll 1 \tag{9}$$

B. Free Fall

The dynamics of the ball during free fall are given by

$$\dot{S} = F(S) = A_S\, S + g \tag{10}$$

$$A_S = \begin{bmatrix} 0 & 1 & 0 & 0 & 0 \\ 0 & 0 & 0 & 0 & 0 \\ 0 & 0 & 0 & 0 & 0 \\ 0 & 0 & 0 & 0 & 1 \\ 0 & 0 & 0 & 0 & 0 \end{bmatrix} \quad g = \begin{bmatrix} 0 \\ 0 \\ 0 \\ 0 \\ -\gamma \end{bmatrix}. \tag{11}$$

Since the perturbations are small, we can approximate the solution to (10) given (9) to first order using a Taylor series expansion. We omit the higher order terms. We further identify the perturbations s_1 at nominal impact time $\bar{T}_1$ as

$$S_1 = S\big(\bar{T}_1, \bar{S}_0\big) + \left.\frac{\partial S\big(\bar{T}_1, S_0\big)}{\partial S_0}\right|_{\bar{S}_0} s_0 \tag{12}$$

$$\cancel{\bar{S}_1} + s_1 = \cancel{S\big(\bar{T}_1, \bar{S}_0\big)} + M_{01} s_0. \tag{13}$$

The Jacobian M_{01} describes the linear mapping of s_0 to s_1 over the free fall.

C. Impact

Due to the introduced perturbations, the impact does not occur at the nominal impact time $\bar{T}_1$, but at $T_2 = \bar{T}_1 + \tau$. Before we can apply the impact function, we have to approximate the ball and paddle state at T_2.

1) Impact States: We derive the motion of the ball for the impact time deviation $\tau = t - \bar{T}_1$. We can reuse (10) with the initial conditions (12), the ball state at nominal impact time $\bar{T}_1$ to get $S(\tau, S_1)$.

We introduce the paddle state $P = (x, \dot{x}, \omega_y, z, \dot{z})$. The paddle motion in τ is the solution to

$$\begin{aligned} P(\tau = 0) &= \bar{P}_1 \\ \dot{P}(\tau) &= G\big(P(\tau)\big). \end{aligned} \tag{14}$$

The paddle dynamics are given by

$$\begin{aligned} G(P) = \dot{P} &= A_P\, P + a \\ A_P &= A_S \\ a &= \begin{bmatrix} 0 & 0 & 0 & 0 & a_P \end{bmatrix}^T. \end{aligned} \tag{15}$$

We approximate the motion of the ball and paddle to first order in τ. Note that to first order, $\dot{S}(\tau, S_1)\ \tau = \dot{\bar{S}}_1\, \tau$.

$$\begin{aligned} S_2^- &= \bar{S}_1 + s_1 + \dot{\bar{S}}_1\, \tau \\ &= \bar{S}_1 + s_2^- \\ P_2^- &= \bar{P}_1 + \dot{\bar{P}}_1\, \tau \\ &= \bar{P}_1 + p_2^-, \end{aligned} \tag{16}$$

where p is the perturbation of the nominal paddle state.

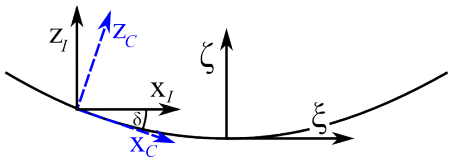

Fig. 3. Paddle Shape, $\zeta = (c/2)\ \xi^2$, and Impact *CS*

2) Impact Condition Function: We solve the general impact condition function Δ for τ using the approximations (16). We approximate Δ to first order in S, P about $\bar{S}_1, \bar{P}_1$.

$$\begin{aligned}\Delta\left(S_2^-, P_2^-\right) &= \cancel{\Delta\left(\bar{S}_1, \bar{P}_1\right)} \\ &\quad + \left.\frac{\partial \Delta\left(S,P\right)}{\partial S}\right|_{\bar{S}_1,\bar{P}_1} s_2^- \\ &\quad + \left.\frac{\partial \Delta\left(S,P\right)}{\partial P}\right|_{\bar{S}_1,\bar{P}_1} p_2^- \qquad (17)\\ 0 &= T_S\, s_2^- + T_P\, p_2^- \\ &= T_S\, \left(s_1 + \dot{\bar{S}}_1\, \tau\right) + T_P\, \dot{\bar{P}}_1\, \tau \qquad (18)\end{aligned}$$

T_S, T_B are the Jacobians of Δ for the ball and paddle perturbations. We solve (18) for τ:

$$\tau = -\left(T_S\, \dot{\bar{S}}_1 + T_P\, \dot{\bar{P}}_1\right)^{-1}\, T_S\, s_1. \qquad (19)$$

For the specific system analyzed, we use the following impact condition:

$$\begin{aligned}\Delta\left(S,P\right) &= i_S\, S - i_P\, P - R \\ i_S = i_P &= \begin{bmatrix}0 & 0 & 0 & 1 & 0\end{bmatrix},\end{aligned} \qquad (20)$$

where R is the ball radius. We neglect the paddle's shape in the impact condition. Δ just compares the z-coordinates of the ball and paddle. An impact occurs if $\Delta = 0$. Since the specific impact condition function is already linear, we get $T_S = -T_P = i_S$.

3) Impact Location: Due to the perturbations, the ball does not hit the paddle in its center at $x = \xi = 0$. The curvature of the paddle and the x-coordinate at impact determine the angle δ at which the impact coordinate system (*CS*) C is in respect to the inertial *CS* I, see Fig. 3.

The impact function is applied in the impact *CS* C; we define the rotation matrix A_{CI} that rotates a vector from I to C.

4) Impact Model: For the vertical impact velocities, we use Newton's impact laws assuming the ratio of the ball's mass to the paddle's mass to be small; the ratio for the robot prototype is 3×10^{-4}.

$$\dot{z}_S^+ = -e_z \dot{z}_S^- + (1 + e_z)\dot{z}_P, \qquad (21)$$

where $\dot{z}_S$ and $\dot{z}_P$ are the vertical velocities of the ball and paddle, respectively. For the horizontal directions and spin, we use the impact model derived in [21]. The horizontal *CR* e_x is defined as:

$$e_x = -\frac{\dot{x}^+ - R\,\omega_y^+}{\dot{x}^- - R\,\omega_y^-}. \qquad (22)$$

R is the ball radius. e_x relates the velocity of the contact point of the ball over the impact. The values of e_x range from -1 to 1.

Combined with conservation of angular momentum and (21), we obtain the following impact function:

$$\Gamma\left(S,P\right) = S^+ = C_S\, S^- + C_P\, P^-. \qquad (23)$$

C_S, C_P are the mappings of the pre-impact ball and paddle state to the post-impact ball state, respectively. Note that (23) is defined in the impact coordinate system.

$$\begin{aligned}C_S &= \begin{bmatrix}1 & 0 & 0 & 0 & 0\\ 0 & 1-k & kR & 0 & 0\\ 0 & \alpha & 1-R\alpha & 0 & 0\\ 0 & 0 & 0 & 1 & 0\\ 0 & 0 & 0 & 0 & -e_z\end{bmatrix} \\ C_P &= \begin{bmatrix}0 & 0 & 0 & 0 & 0\\ 0 & k & 0 & 0 & 0\\ 0 & -\alpha & 0 & 0 & 0\\ 0 & 0 & 0 & 0 & 0\\ 0 & 0 & 0 & 0 & e_z+1\end{bmatrix} \\ \alpha &= \frac{e_x+1}{1.4R},\ k = \frac{e_x+1}{3.5},\ \beta = k - 1 - e_z\end{aligned} \qquad (24)$$

5) Impact Function: (16) and (19) define the ball and paddle state before impact. We apply the impact function (23) on the rotated vectors and rotate the result back into the inertial frame. We define

$$\Gamma_I\left(S_2^-, P_2^-\right) := A_{CI}^T \Gamma\left(A_{CI} S_2^-, A_{CI} P_2^-\right). \qquad (25)$$

Γ_I represents the impact function acting directly in I. We approximate Γ_I to first order to obtain the post-impact ball state.

$$\begin{aligned}S_2^+ &= \Gamma_I\left(\bar{S}_2^-, \bar{P}_2^-\right) \\ &\quad + \left.\frac{\partial \Gamma_I\left(S,P\right)}{\partial S}\right|_{\bar{S}_2^-,\bar{P}_2^-} s_2^- \\ &\quad + \left.\frac{\partial \Gamma_I\left(S,P\right)}{\partial P}\right|_{\bar{S}_2^-,\bar{P}_2^-} p_2^- \\ &= \bar{S}_2^+ + s_2^+ \end{aligned} \qquad (26)$$

D. Free Fall until Apex

After the impact, the ball is in free fall until the nominal apex time $\bar{T}_3$. The free fall is analogous to Section III-B. We reuse M_{01} from (13) to map the perturbations at $\bar{T}_1 + \tau$ to $\bar{T}_3 + \tau$. We get

$$S\left(\bar{T}_3 + \tau\right) = \bar{S}_3 + M_{01}\, s_2^+. \qquad (27)$$

In order to obtain the ball state at the nominal apex time $\bar{T}_3$, we compensate for τ analogous to (16):

$$S_3 = \bar{S}_3 + M_{01}\, s_2^+ - \dot{\bar{S}}_3\, \tau. \qquad (28)$$

We combine (13), (16), (19), (26), (28) and obtain the matrix M_{03} which maps the initial perturbations s_0 over a single bounce.

$$s_3 = M_{03}\, s_0 \qquad (29)$$

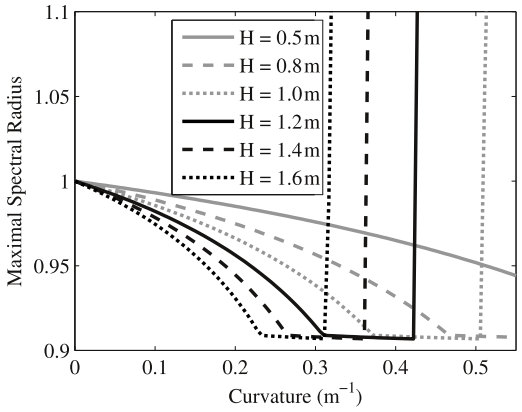

Fig. 4. $\max_{e_x} \rho(A_x)$ for various Apex Heights H, $e_z = 0.8$

For the specific system, the mapping M_{03} is a block-diagonal matrix with blocks corresponding to $x, \dot{x}, \omega_y$ and $z, \dot{z}$.

$$M_{03} = \begin{bmatrix} A_x & 0 \\ 0 & A_z \end{bmatrix}, \tag{30}$$

with

$$A_x = \begin{bmatrix} \frac{2c\beta\gamma\bar{T}_1^2}{e_z+1} + 1 & \bar{T}_1\left(\frac{2c\beta\gamma\bar{T}_1^2}{e_z+1} - k + 2\right) & kR\bar{T}_1 \\ \frac{2c\beta\gamma\bar{T}_1}{e_z+1} & \frac{2c\beta\gamma\bar{T}_1^2}{e_z+1} - k + 1 & kR \\ -\frac{2c\gamma\alpha\bar{T}_1}{e_z+1} & \alpha - \frac{2c\gamma\alpha\bar{T}_1^2}{e_z+1} & 1 - R\alpha \end{bmatrix}$$

$$A_z = \begin{bmatrix} \frac{a_P(e_z+1)^2+\gamma\left(e_z^2+1\right)}{2\gamma} & \frac{\left(\gamma(e_z-1)^2+(e_z+1)^2 a_P\right)\bar{T}_1}{2\gamma} \\ \frac{(e_z+1)^2(\gamma+a_P)}{2\gamma\bar{T}_1} & \frac{a_P(e_z+1)^2+\gamma\left(e_z^2+1\right)}{2\gamma} \end{bmatrix}.$$

IV. DESIGN PARAMETERS

With the mapping M_{03}, we analyze the local stability of the system. The goal is to find stabilizing values for the unknown design parameters curvature c and paddle acceleration a_P for a range of apex heights and ball properties.

We analyze the spectral radius ρ of M_{03} to determine the stability of the system; if ρ is smaller than one, the system is stable. The spectral radius of a matrix is defined as $\rho(A) := \max_i |\lambda_i(A)|$, where λ_i is the i-th eigenvalue of A.

Since A_x is independent of a_P and A_z is independent of c, we can determine the two design parameters independently.

A. Paddle Curvature

Stability of the ball's horizontal perturbations can be achieved by choosing an appropriate paddle curvature as sketched in Fig. 3. We evaluate the spectral radius ρ of A_x over a range of apex heights and ball properties. We find that ρ is sensitive to the apex height. The *CR* e_z appears in A_x, but has negligible influence on stability.

In Fig. 4 we show the maximum spectral radius of A_x over the range $e_x \in [-0.5, 0.5]$ as a function of c for various apex heights H.

We set the design specification for the first robot prototype to juggle at heights up to $1.2\,\mathrm{m}$. Therefore, choosing $c = 0.36\,\mathrm{m}^{-1}$ satisfies the stability requirement. We further predict that the ball should fall off the paddle for heights larger $1.4\,\mathrm{m}$.

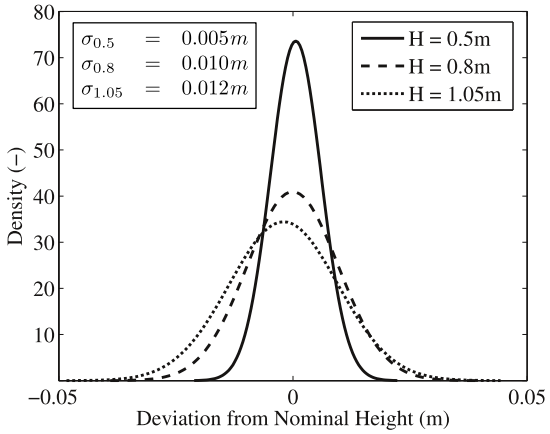

Fig. 5. Fitted Gaussians for Apex Height Deviations with Standard Deviations σ_H

B. Paddle Acceleration

Stability of the apex height is achieved by the proper paddle acceleration. It has been shown in previous work that a negative acceleration is stabilizing [8], [11], [12].

The spectral radius of A_z is independent of the apex height. For a range of $a_P \in [-1, -10]\ \mathrm{ms}^{-2}$, the spectral radius is constant and smaller than one for any given $e_z \in [0.7, 0.9]$. We choose $a_P = -\gamma/2$ which lies in the center of the stable region.

V. ROBOT PROTOTYPE

We built a robot prototype (Fig. 1) with the determined design parameters. It consists of a linear motor actuating a solid aluminum paddle. The paddle was CNC-milled to the desired shape and has a diameter of $0.3\,\mathrm{m}$. We chose the motor to be able to continuously juggle balls at heights up to at least $1.2\,\mathrm{m}$ and e_z larger 0.7 (tennis ball).

The quadratic trajectory of the paddle is driven by a servo controller. A high level state machine running on a D-Space real time control system [22] provides the profile parameters to the controller and is timing the motion.

For given parameters e_z, a_P and H, the paddle's trajectory is fully defined except the duration the paddle is decelerating around the nominal impact time. We determine this duration by assuming an upper bound for a static error in e_z.

A. Impact of Ball Properties on Performance

After some experiments with different balls, we observed that the main source of noise in the measured impact times and locations are stochastic deviations of the impact parameters, i.e. ball roundness and *CR*. High precision balls, which are specifically manufactured to have very precise roundness for valve applications, introduce the least amount of noise. Only these high precision balls allow the robot to juggle at apex heights larger than $0.6\,\mathrm{m}$. Less precise balls (Superball, table tennis ball, etc.) generate too much noise in the horizontal degrees of freedom and eventually fall off at larger apex heights. We show a ball comparison in the video submitted with this paper.

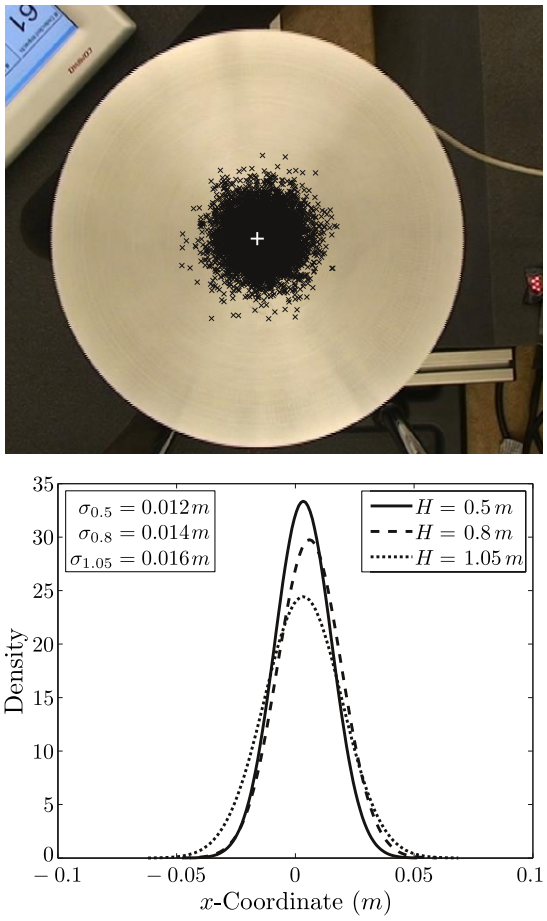

Fig. 6. Impact Location Data for Paddle Curvature $c = 0.36\ \mathrm{m}^{-1}$. Top: Accumulated Impact Locations (x) and Paddle Center (+) for $H = 1.05$ m. Bottom: Fitted Impact Coordinate Distributions.

B. Measurements

A piezo film strain gage attached to the paddle acting as a contact microphone lets us measure the impact times. An encoder on the linear motor provides information about the paddle position. We measure the impact locations using a video camera mounted above the paddle. We collected data at three different nominal apex heights: $0.5, 0.8$ and 1.05 m. In the three experiments, we recorded a total of $5301, 4549$ and 5789 consecutive impacts, respectively.

1) Apex Height: From the paddle positions of two consecutive impacts and the impact time difference, we estimate the apex height of the ball. In Fig. 5, we show the Gaussian distributions fitted to the data.

2) Impact Locations: In Fig. 6, we show the results of the impact location measurements. The distributions are rather narrow. However, this performance can only be achieved with a precision ball. For the measurements presented, we used a solid PA-6.6 ball with a diameter of 0.012 m.

The measurements confirm the assumption that x, ω_y and y, ω_x of the ball are uncorrelated. The covariance matrix of n = 5789 measured impact coordinates $X = (x, y)$ with $x, y \in \mathbb{R}^{n\times 1}$ for $H = 1.05$ m is

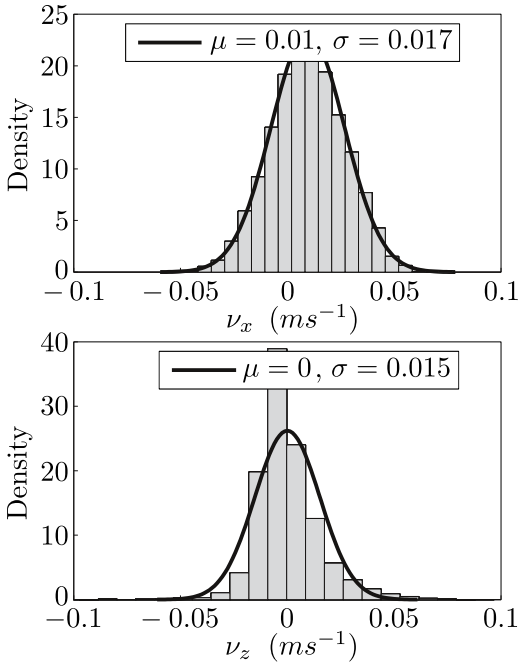

Fig. 7. Noise Histograms and fit Gaussians for $H = 1.05$ m.

$$10^{-3} \cdot \begin{bmatrix} 0.267 & -0.003 \\ -0.003 & 0.273 \end{bmatrix} \ \mathrm{m}^2. \tag{31}$$

We measured small non-zero means in the impact location distributions (Fig. 6). This is due to a slightly misleveled paddle and would be zero for a perfectly leveled paddle.

C. Parameter Identification

From the impact times, paddle positions and velocities at impact, we identify e_z from the data. The parameter slightly decreases with increasing heights and lies in the interval $e_z \in [0.79, 0.82]$.

We estimate the horizontal impact parameter e_x from the data by minimizing the deviation of the predicted post-impact horizontal velocities to the measured velocities. As we have no measure of the ball's spin, this proves to be difficult; we obtain three different values for the three impact heights. For $H = 1.05$ m, we even obtain $e_x = 1.2$, which lies outside the range of possible values for e_x. Without measuring the spin of the ball, we cannot properly estimate e_x.

D. Noise Identification

We identify the noise as the deviations from the measured to the predicted post-impact velocities. For the prediction, we use the linear model derived in Section III with the identified parameters of e_z. For the unknown parameter e_x, we choose a fixed value of $e_x = 0.2$, assuming a gripping ball less elastic than a Superball [21].

$$S^+_{2,meas} = S^+_{2,pred} + \nu, \tag{32}$$

with $\nu = (0, \nu_x, 0, 0, \nu_z)^T$. We also measure the noise in y-direction. This is straightforward, since this direction

is independent of the others (31). We can extend the linear model to include the y-direction.

Since we cannot measure the ball's spin, we assume zero spin at all times and capture the influence of spin on the system in the noise. In Fig. 7 we show fitted Gaussian distributions to the measurement histograms of ν_x, ν_z. The histogram of ν_z appears less Gaussian since the actual paddle deceleration is not perfectly linear.

We analyze the auto-correlation sequences of the noise data and learn that a white noise model is a good approximation to the measured noise.

VI. REFINING THE DESIGN PARAMETERS

Now that we characterized the noise introduced into the system as white noise, we can use the H_2 norm to refine the design parameters. An interpretation of the H_2 norm is, roughly speaking, the gain of a system when the input is white noise [1]. By minimizing the H_2 norm, we can find the design parameters that maximally reject the noise and improve the performance of the system.

Analogous to the stability analysis in Section IV, we can optimize the design parameters c and a_P independently as M_{03} is block diagonal and the noise introduced in the vertical and horizontal directions only impacts the respective degree of freedoms.

A. Optimized Paddle Curvature

We want to find the paddle curvature parameter c that minimizes the H_2 norm over a range of ball properties. In order to apply the norm to the system, we have to derive the input-output representation of the system for the horizontal directions. The x and y directions are independent, hence the paddle curvature minimizing the two dimensional system also minimizes the three dimensional one. The state is $s_x = (x, \dot{x}, \omega_y)$. The system output w_x is equivalent to the impact location on the paddle, which is what we want to keep small. The input is $d_x = \nu_x$, the post-impact velocity deviation.

$$\begin{aligned} s_x(k+1) &= A_x s_x(k) + B_x d_x(k) \\ w_x(k) &= C_x s_x(k) \end{aligned} \tag{33}$$

We call this LTI system G_x. It is discrete with a sample time of $2\bar{T}_1$. The matrices are

$$B_x = \left[\bar{T}_1, 1, 0\right]^T \qquad C_x = \left[1, \bar{T}_1, 0\right]. \tag{34}$$

We find $c = 0.25$ from

$$\min_c \underbrace{\max_{e_x} \|G_x\left(c, e_x\right)\|_2}_{J(c)} \tag{35}$$

for $H = 1.05$ m and $e_z = 0.8$. Since we could not identify the parameter e_x from the measurements, we minimize a worst case value of the H_2 norm over the range $e_x \in [-0.5, 0.2]$. This range captures a slipping to gripping impact of the ball which is less elastic than a Superball, see [21].

TABLE I
IMPACT LOCATION STANDARD DEVIATIONS

H	$c = 0.36\ \mathrm{m}^{-1}$	$c = 0.24\ \mathrm{m}^{-1}$	Change
0.5 m	0.0120 m	0.0130 m	9.1%
0.8 m	0.0134 m	0.0141 m	4.8%
1.05 m	0.0163 m	0.0147 m	-10.1%

1) Results: We manufactured a paddle with a slightly smaller $c = 0.24\ \mathrm{m}^{-1}$, which is acceptable as $J(0.24)$ and $J(0.25)$ are both equal to 1.72 for unscaled input. We measured the impact locations using the new paddle and show a comparison of the measured standard deviations of the impact x-coordinate in Table I.

The system performance with $c = 0.24\ \mathrm{m}^{-1}$ decreases for lower heights; we can accept this as increased impact location deviations are more likely to cause the ball to fall off at larger heights.

We achieve larger apex heights with the new paddle; this is predicted in Fig. 4. For $c = 0.24\ \mathrm{m}^{-1}$, the robot juggles at heights up to 2.1 m. We show this in the video submitted with the paper.

B. Optimized Paddle Acceleration

Analogous to the paddle shape optimization, we can optimize the paddle acceleration a_P. We build the input-output system for the vertical directions. The state vector becomes $s_z = (z, \dot{z})$. The input is $d_z = \nu_z$, the post-impact velocity deviation. We seek to minimize the output w_z, which is equivalent to the z-coordinate of s_1, the perturbation in height at nominal impact time.

$$\begin{aligned} s_z(k+1) &= A_z s_z(k) + B_z d_z(k) \\ w_z(k) &= C_z s_z(k) \end{aligned} \tag{36}$$

We call this discrete LTI system with sample time $2\bar{T}_1$ G_z. The matrices are

$$B_z = \left[\bar{T}_1, 1\right]^T \qquad C_z = \left[1, \bar{T}_1\right]. \tag{37}$$

We obtain $a_P = -4.95\ \mathrm{ms}^{-2}$ from

$$\min_{a_P} \|G_z\left(a_P\right)\|_2 \tag{38}$$

with $H = 1.05$ and $e_z = 0.8$. This value is almost identical to the stabilizing value we chose in Section IV of $-4.9\ \mathrm{ms}^{-2}$.

VII. H_2 OPTIMAL CONTROLLER FOR APEX

Since the horizontal degree of freedoms are decoupled from the vertical ones, we cannot actively control the ball's horizontal impact location. However, we can use feedback control to increase the vertical performance. We design a feedback controller K that minimizes the H_2 norm of the closed-loop system.

We use τ, the impact time deviation as feedback; the contact microphone we attached to the paddle provides this measurement. As control action, we use the deviation from nominal impact height and velocity of the paddle, thus

$u = (u_z, u_{\dot{z}})^T$. In order to design the controller for G_z, we extend the system (36) to include τ and u:

$$\begin{aligned} q(k+1) &= \tilde{A}q(k) &&+\tilde{B}_1 d_z(k) &&+\tilde{B}_2 u(k) \\ w_z(k) &= \tilde{C}_1 q(k) &&+\tilde{D}_{11} d_z(k) &&+\tilde{D}_{12} u(k) \\ \tau(k) &= \tilde{C}_2 q(k) &&+\tilde{D}_{21} d_z(k) &&+\tilde{D}_{22} u(k). \end{aligned} \tag{39}$$

For determining $u(k)$, we only have the previous impact time. We capture this measurement delay in the system dynamics by extending the state to $q = \left[s_z^T, \tau\right]^T$. This allows us to calculate $u = K\tau$.

$$\begin{aligned} \tilde{A} &= \begin{bmatrix} A_z & 0 \\ C_\tau & 0 \end{bmatrix} & \tilde{B}_1 &= \begin{bmatrix} B_z \\ 0 \end{bmatrix} & \tilde{B}_2 &= \begin{bmatrix} B_u \\ D_\tau \end{bmatrix} \\ \tilde{C}_1 &= \begin{bmatrix} C_z & 0 \end{bmatrix} & \tilde{C}_2 &= \begin{bmatrix} 0 & 0 & 1 \end{bmatrix} \\ \tilde{D}_{11} &= \tilde{D}_{12} = 0 & \tilde{D}_{21} &= \tilde{D}_{22} = 0 \end{aligned} \tag{40}$$

We already derived C_τ in (19). We can derive D_τ in the perturbation analysis by adding u to p_2^- in (16).

With the system established, we can find the controller matrix K that minimizes the closed-loop H_2 norm from input d_z to w_z. For $H = 1.05\,\mathrm{m}$, $e_z = 0.8, a_P = -\gamma/2$ and scaling the input with the measured $\sigma_{\nu z} = 0.015$, we achieve a closed-loop norm of 0.014. Given the same parameters, the open-loop norm is 0.017. We can only reduce the norm by 14% with feedback control. Considering that the measured standard deviations of the apex height distributions are already small (Fig. 5), the improvement is marginal.

Note that by choosing $\tilde{D}_{12} = 0$, we do not constrain the control action. Therefore, the improvement is an upper bound that may not be physically possible; for example, the stroke of the linear motor is limited.

VIII. CONCLUDING REMARKS

We showed that feedback control is not necessary for the apex height. However, feedback control in an adaptive setting as in [23] can relax the a priori knowledge about the *CR* and compensate for the decrease of the *CR* at increasing height. This reduces the required stroke of the linear motor as the mean impact time deviation is eliminated.

We have recently identified that the paddle shape optimization can be improved by considering the fact that the noise amplitude we determined in Section V-D is also a function of the unknown parameter e_x. We are currently working on incorporating this knowledge into the optimization process and plan to manufacture a new paddle in the near future. We will also look into finding a way to reliably estimate the impact parameter e_x.

Lastly, we believe that determining the optimal paddle acceleration experimentally, i.e. by minimizing the measured apex deviations, and comparing the results with [12] would yield interesting insights.

IX. ACKNOWLEDGMENTS

We would like to thank Matthew Donovan for his great help with the mechanical design of the robot. We further thank Angela Schöllig and Sebastian Trimpe for their suggestions that helped improve the controller design and perturbation analysis.

REFERENCES

[1] B. Anderson and J. Moore, *Optimal control: Linear Quadratic Methods*. Prentice-Hall, 1990.
[2] P. J. Holmes, "The dynamics of repeated impacts with a sinusoidally vibrating table," *Journal of Sound Vibration*, vol. 84, pp. 173–189, Sep. 1982.
[3] N. Tufillaro, T. Abbot, and J. Reilly, *An experimental approach to nonlinear dynamics and chaos*. Addison-Wesley, 1992.
[4] M. Bühler, D. E. Koditschek, and P. J. Kindlmann, "A simple juggling robot: Theory and experimentation," in *Proceedings of the First International Symposium on Experimental Robotics*, 1990.
[5] ——, "Planning and control of robotic juggling and catching tasks," *I. J. Robotic Res.*, vol. 13, no. 2, pp. 101–118, 1994.
[6] ——, "A family of robot control strategies for intermittent dynamical environments," in *Proceedings of the International Conference on Robotics and Automation*, Scottsdale, AZ, 1989.
[7] ——, "A one degree of freedom juggler in a two degree of freedom environment," in *Proceedings of the International Workshop on Intelligent Robots*, Nov. 1988.
[8] S. Schaal and C. Atkeson, "Open loop stable control strategies for robot juggling," in *Proceedings of the International Conference on Robotics on Robotics and Automation*, May 1993.
[9] R. Ronsse, P. Lefevre, and R. Sepulchre, "Timing feedback control of a rhythmic system," in *Proceedings of the Conference on Decision and Control and European Control Conference (CDC-ECC)*, 2005.
[10] ——, "Sensorless stabilization of bounce juggling," *IEEE Transactions on Robotics*, vol. 22, no. 1, pp. 147–159, Feb. 2006.
[11] R. Ronsse and R. Sepulchre, "Feedback control of impact dynamics: the bouncing ball revisited," in *Proceedings of the Conference on Decision and Control*, Dec. 2006.
[12] R. Ronsse, P. Lefevre, and R. Sepulchre, "Rhythmic feedback control of a blind planar juggler," *IEEE Transactions on Robotics*, vol. 23, no. 4, pp. 790–802, Aug. 2007.
[13] T. Vincent, "Controlling a ball to bounce at a fixed height," in *Proceedings of the American Control Conference*, Jun. 1995.
[14] M. M. Williamson, "Designing rhythmic motions using neural oscillators," in *Proceedings of the International Conference on Intelligent Robot and Systems*, 1999.
[15] T. Junge, "One Dimension Robot Juggler," Master's thesis, Massachusetts Institute of Technology, Cambridge, MA, August 2008.
[16] A. A. Rizzi and D. E. Koditschek, "Preliminary experiments in spatial robot juggling," in *Proceedings of the 2nd International Symposium on Experimental Robotics*, London, UK, 1993.
[17] A. Rizzi and D. Koditschek, "Progress in spatial robot juggling," in *Proceedings of the International Conference on Robotics on Robotics and Automation*, May 1992.
[18] A. Rizzi, L. Whitcomb, and D. Koditschek, "Distributed real-time control of a spatial robot juggler," *Computer*, vol. 25, no. 5, pp. 12–24, May 1992.
[19] A. Nakashima, Y. Sugiyama, and Y. Hayakawa, "Paddle juggling of one ball by robot manipulator with visual servo," in *Proceedings of the International Conference on Control, Automation, Robotics and Vision*, Dec. 2006.
[20] R. P. Ringrose, "Self-stabilizing running," Ph.D. dissertation, Massachusetts Institute of Technology, Cambridge, MA, 2008.
[21] R. Cross, "Grip-slip behavior of a bouncing ball," *American Journal of Physics*, vol. 70, no. 11, pp. 1093–1102, 2002.
[22] http://www.dspace.de/.
[23] A. Zavala-Río and B. Brogliato, "Direct adaptive control design for one degree-of-freedom complementary-slackness jugglers," *Automatica*, vol. 37, pp. 1117–1123(7), July 2001.